CHAPTER 4

OPTIMIZATION OF BACTERIAL CELLULOSE PRODUCTION FROM THAI RED TEA KOMBUCHA USING CENTRAL COMPOSITE DESIGN IN RESPONSE SURFACE METHODOLOGY

4.1 Abstract

This study optimized bacterial cellulose (BC) production from Thai red tea kombucha using response surface methodology (RSM) with a central composite design (CCD), based on previous data. Thirty-four runs evaluated the effects of sucrose–glucose ratio, tea concentration, and ethanol concentration on BC wet yield, dry yield, and water-holding capacity (WHC), with emphasis on wet yield. Despite some limitations, the model showed acceptable predictive accuracy. During optimization, the software generated 53 formulations, from which three—RTC-V1 (recommended), RTC-V46 (highest predicted yield), and RTC-V53 (lowest predicted yield)—were selected for validation. Observed yields and WHC values closely matched predictions, confirming model reliability. RTC-V1 (7.97% (w/v) sucrose, 2.03% (w/v) glucose, 1.41% (w/v) tea, 1.56% (v/v) ethanol) achieved a wet BC yield of 621.71 ± 24.06 g/L, a 238% increase over the RTC-SGlu formulation. The optimized BC was characterized by SEM, FTIR, XRD, TGA, and nanoindentation, confirming a uniform nanofiber network, cellulose I structure with high crystallinity (83.23–85.97%), thermal stability, and strong mechanical properties. These findings support the effectiveness of CCD-based RSM for scalable, high-quality BC production.

Keywords: Bacterial cellulose optimization, Thai red tea kombucha, Composite central design (CCD), Fermentation process, BC production.

4.2 Introduction

Bacterial cellulose (BC) is a microbial exopolysaccharide produced predominantly by *Komagataeibacter* sp. Compared to plant-derived cellulose, BC is free from lignin and hemicellulose and possesses superior characteristics, including high purity, crystallinity, tensile strength, water-holding capacity (WHC), and biocompatibility. These properties make BC a promising material in various sectors, such as food, biomedical, and packaging industries (Azeredo et al. 2019b; Barja 2021b; Bizeau and Mertz 2021; Padmanabhan et al. 2023).

Among sustainable production methods, kombucha fermentation has attracted growing interest for BC production. Kombucha, a fermented tea beverage, is produced by a SCOBY in a sugar-enriched tea medium. During fermentation, the microbial community metabolizes the carbon source and forms a cellulose pellicle on the surface of the liquid. This process presents a natural, cost-effective, and scalable approach to BC production, utilizing readily available substrates such as tea and sugar (Cavicchia and de Almeida 2022; Ramírez Tapias et al. 2022; Charoenrak et al. 2023).

BC production during fermentation is influenced by several factors, including the type and concentration of tea, the ratio of carbon sources (glucose and sucrose), ethanol supplementation, and fermentation parameters such as time, pH, and temperature. Glucose serves as the primary carbon source for BC biosynthesis, whereas sucrose must first be hydrolyzed, potentially affecting the fermentation rate. Tea provides essential nutrients—including nitrogen, polyphenols, and micronutrients—that support microbial growth and activity. Low concentrations of ethanol have been shown to enhance BC yield, though higher levels may have inhibitory effects (Kazemi et al. 2015; Molina-Ramírez et al. 2018b; Fei et al. 2023).

To maximize BC productivity and reduce production costs, statistical optimization approaches like Response Surface Methodology (RSM) have been widely employed. RSM is an effective tool to evaluate the effects and interactions of multiple variables on a given response. Specifically, Central Composite Design (CCD) within the

RSM framework offers an efficient experimental layout for identifying optimal conditions with a reduced number of runs. For example, the Box-Behnken design has been used to optimize temperature, pH, and agitation speed, resulting in a threefold increase in BC yield (Pandey et al. 2024). Likewise, Plackett–Burman and RSM were used to optimize BC production by *K. rhaeticus* N1 MW32270, increasing the yield from 4.3 g/L to 9.2 g/L (Mohammad et al. 2021). In another study, CCD was applied using low-cost nutrient sources like molasses, ethanol, corn steep liquor (CSL), and ammonium sulfate, leading to a 6.3-fold increase in productivity compared to the standard Hestrin–Schramm (HS) medium (Rodrigues et al. 2019). Optimization of the growth medium for *A. senegalensis* MA1 using CCD-RSM increased BC production up to 20 times relative to unoptimized HS medium (Aswini et al. 2020). These findings highlight the effectiveness of RSM in elucidating complex parameter interactions and improving BC production outcomes.

Despite the promising use of alternative substrates for BC production, limited studies have explored Thai red tea kombucha as a fermentation medium. Thai red tea is commercially popular and contains both natural polyphenols and artificial colorants such as FD&C Yellow No. 6 (INS 110), which may influence microbial growth and cellulose biosynthesis. Furthermore, flavored teas used in this context may introduce additional bioactive compounds or fermentation modulators.

This study aims to optimize BC production from Thai red tea kombucha through CCD-RSM. The key variables examined include tea concentration, sucrose-to-glucose ratio, and ethanol content. Based on previous work, the fermentation was conducted at a tea concentration of 2%, ethanol 1%, and a carbon source mixture totaling 10% under static conditions for 15 days at pH ~5.20. The objectives are to (i) maximize wet and dry BC yield and WHC, (ii) verify the fit between predicted and actual results, and (iii) characterize the optimized BC using SEM, FTIR, XRD, TGA, and nanoindentation to assess its structural, thermal, and mechanical properties. These

findings aim to support the development of a cost-effective, reproducible, and industrially scalable BC production method for functional and packaging applications.

4.3 Materials and Methods

The materials and equipment used in this stage include commercial kombucha starter (SCOBY) bought from Neo Cold Brew Shop (online market, Thailand), sucrose, Thai red tea-vanilla flavor (*ChaTraMue* brand), sucrose, glucose, ethanol, sodium hydroxide (NaOH), Hydrochloric acid (HCl), Reverse osmosis (RO) water, Deionized (DI) water, cheese cloth, coffee filter, glass jar, funnel, autoclave, laminar air flow, laboratory glassware, analytical balance, incubator, pH-meter (Oakton, pH 700), refractometer, oven dryer (XUE058, FRANCE ETUVES), FT-IR (Bruker VERTEX 70), XRD (Bruker D8 Advance), SEM (FESEM) (Zeiss, AURIGA, Germany), HPLC (Hitachi Chromaster), and, nano-indenter (NanoTest Vantage system, Micro Materials Limited in Wrexham, UK).

4.3.1 Experimental Design Using CCD of RSM

The optimization of BC (BC) production was carried out using Response Surface Methodology (RSM) with a Central Composite Design (CCD), developed using Design-Expert 11 software. The selection of independent variables and their ranges was based on findings from previous experiments (**Chapter 3**). The optimization aimed to maximize BC yield (g/L, wet and dry basis) and water holding capacity (WHC).

Three independent variables were selected: Thai red tea concentration (1–3%, with 2% as the center point), ethanol concentration (0–2%, with 1% as the center point), and the ratio of sucrose to glucose as the carbon source, with a fixed total sugar concentration of 10%. The goal was to determine the optimal sucrose-to-glucose ratio within this fixed concentration. These ranges were chosen based on previous results showing that a 1:1 ratio (5% sucrose + 5% glucose) yielded favorable outcomes.

The cultivation conditions were kept constant throughout the optimization: unadjusted initial pH (~5.20), static fermentation, room temperature, and a 15-day fermentation time. Although a 14-day fermentation had previously been found optimal, a 15-day duration was used in this study to maintain consistency with earlier experimental protocols and to allow slight flexibility in timing without affecting BC quality. The variables and their levels used in the experimental design are summarized in **Table 4.1**, and the full design matrix generated by the software is presented in **Table 4.2.**

The following is further information on the optimization methods:

Study Type : Response Surface
Subtype : Randomized
Design Type : Central Composite
Runs : 34
Design Model : Quadratic
Blocks : No Blocks

Table 4.1 The factors used in the design of experiment for BC production from RTC kombucha fermentation and its value

F	Name	Units	Type	Min.	Max.	CL	CH	Mean	SD
A	[Sucrose]	%	Numeric	0.00	10.00	-1 ↔ 2.03	+1 ↔ 7.97	5.00	2.70
B	[Tea]	%	Numeric	1.00	3.00	-1 ↔ 1.41	+1 ↔ 2.59	2.00	0.54
C	[Ethanol]	%	Numeric	0.00	2.00	-1 ↔ 0.41	+1 ↔ 1.59	1.00	0.54

F = Factors, Min. = Minimum, Max. = Maximum, Cl = Coded Low, CH = Coded high, SD = Standard Deviation.

Table 4.2 Design of experiment for the optimization of BC production from RTC kombucha fermentation

		Factors			Responses		
Std	**Run**	**[Sucrose]***	**[Tea]**	**[Ethanol]**	**Wet yield**	**Dry yield**	**WHC**
		%	**%**	**%**	**g/L**	**g/L**	**g/g**
2	1	2.0270	1.4054	0.4054			
17	2	0	2	1			
11	3	7.9730	1.4054	1.5946			
13	4	2.0270	2.5946	1.5946			
32	5	5	2	1			
1	6	2.0270	1.4054	0.4054			
34	7	5	2	1			
21	8	5	1	1			
20	9	10	2	1			
16	10	7.9730	2.5946	1.5946			
22	11	5	1	1			
27	12	5	2	2			
7	13	7.9730	2.5946	0.4054			
24	14	5	3	1			
30	15	5	2	1			
12	16	7.9730	1.4054	1.5946			
3	17	7.9730	1.4054	0.4054			
29	18	5	2	1			
25	19	5	2	0			
26	20	5	2	0			
8	21	7.9730	2.5946	0.4054			
23	22	5	3	1			
15	23	7.9730	2.5946	1.5946			

Table 4.2 Design of experiment for the optimization of BC production (Continued)

		Factors			Responses		
Std	**Run**	**[Sucrose]***	**[Tea]**	**[Ethanol]**	**Wet yield**	**Dry yield**	**WHC**
		%	**%**	**%**	**g/L**	**g/L**	**g/g**
28	24	5	2	2			
19	25	10	2	1			
9	26	2.0270	1.4054	1.5946			
18	27	0	2	1			
6	28	2.0270	2.5946	0.4054			
10	29	2.0270	1.4054	1.5946			
33	30	5	2	1			
31	31	5	2	1			
14	32	2.0270	2.5946	1.5946			
4	33	7.9730	1.4054	0.4054			
5	34	2.0270	2.5946	0.4054			

*) *Total carbon source is 10%, the glucose was added until total carbon source is 10%. Std (standard order)*

4.3.2 Laboratory Experimentation

For each experimental run, Thai red tea kombucha fermentation was prepared according to the designed formula. The fermentation process was conducted under controlled conditions, and the BC produced was harvested after a predetermined incubation period. The harvested BC samples were washed, purified, and analyzed for wet yield (g), dry yield (g), and water holding capacity (WHC, g water/g cellulose).

1) Regeneration of Kombucha Starter

A 480-ml jar was filled with 40g of sucrose and RTC tea extract, prepared by brewing 4g of tea with 360 ml of hot water (T = ±90°C). The tea was filtered using coffee filter paper, placed in a jar filled with sucrose, stirred, and sterilized

by autoclaving (P=1.2 psi, T = 121oC, t = 20 minutes). The mixture was then cooled to near room temperature (30–35°C), inoculated with 40 ml of the previous starter, and fermented for 14 days.

2) Preparation of Medium and Fermentation

A total of 34 jars were prepared, each containing 10 g of a sucrose and glucose mixture, as specified in **Table 4.2**. To each jar, 90 ml of Thai red tea extract was added according to the treatments outlined in **Table 4.2**, and the mixture was stirred until the sugar completely dissolved. The tea extract was prepared by brewing the specified amount of tea in hot water at approximately 90 °C for about 15 minutes, followed by filtration using coffee filter papers. The jars were covered with two layers of cheesecloth and sterilized in an autoclave at 1.2 psi and 121 °C for 20 minutes. After sterilization, the mixture was allowed to cool to 30–35 °C. Once cooled, the appropriate amount of ethanol was added (as shown in **Table 4.2**), and each jar was inoculated with 10 ml of the culture starter. The mixtures were thoroughly mixed and allowed to ferment for 15 days at a temperature of 30 °C under static cultivation conditions.

3) Harvesting and Purification of BC

After around 15 days of fermentation, the BC was separated by lifting it using tweezers and drained for about 10 minutes. The BC was then weighed to determine the wet gross weight, heated in boiling water (± 90–95°C) for about 30 minutes, and drained for about 10 minutes. The BC was then heated at ± 90°C in the alkaline solution (NaOH, 2%) for 120 minutes, drained, rinsed with RO water until the pH was neutral, and washed with DI water (Yanti et al. 2018; Aswini et al. 2020). After that, the BC was then drained for about 10 minutes and weighed to determine the net wet weight. Further, for making the dry samples, the BC sample was then dried using an oven at a temperature of 40°C until it reached a constant weight (Aswini et al. 2020).

4.3.3 Data Analysis and Model Fitting

The response data (wet yield, dry yield, and WHC) were input into the software. Statistical models were developed for each response variable, and their adequacy was evaluated using analysis of variance (ANOVA). Response surfaces and contour plots were generated to visualize the effect of factors and their interactions on BC production.

4.3.4 Optimization and Solution Validation

The optimization module of the software was used to determine the best formula solution for maximizing the desired responses. The predicted optimal conditions were validated by conducting laboratory experiments using the solution formula. The experimental data were compared with the predicted values to validate the optimization model.

4.3.5 Bacterial cellulose characterization

The BC produced using the optimized formula was characterized to confirm its quality and properties. The characterization included yield and WHC, as well as analyses using scanning electron microscopy (SEM), Fourier-transform infrared spectroscopy (FTIR), X-ray diffraction (XRD), thermogravimetric analysis (TGA), and nano-indentation. The detailed methods and procedures for these analyses, including statistical analysis, have been described in Chapter 3 of this thesis.

4.3.6 Statistical Analysis

Analysis of variance was carried out using Ms. Excel software. The differences between the mean values were analyzed using least significant difference (LSD) test and the significance level was set at $P < 0.05$.

4.4 Results and Discussion

4.4.1 Data Analysis of Experimental Design

A total of 34 experimental runs were generated using a CCD as part of the RSM approach. Following a 15-day fermentation, BC samples were purified, and

their wet yield, dry yield, and WHC were determined. The resulting response data were entered into the software for model development and statistical analysis. A summary of the experimental results is presented in **Table 4.3.**

In this study, three response variables—wet yield, dry yield, and WHC—were selected to provide a comprehensive assessment of both BC productivity and quality. Wet yield was considered the primary response, as it represents the total amount of BC produced under each fermentation condition and is directly relevant for industrial and process-scale evaluations. Dry yield and WHC were included as secondary responses to offer additional insight into the structural and functional characteristics of the produced BC. Dry yield reflects the actual amount of cellulose synthesized, independent of water content, and is critical for evaluating true BC productivity. WHC, on the other hand, indicates the material's capacity to retain water, an important functional property for applications in food, cosmetics, biomedical materials, and other moisture-sensitive products. The combination of these three responses allows for a more holistic evaluation of the process, enabling the identification of optimal conditions that not only maximize yield but also ensure desirable material properties suitable for practical applications.

Table 4.3 The data of wet yield, dry yield, and WHC from the laboratory experiment

		Factors			Responses		
STD	**Run**	**Sucrose* (%)**	**Tea (%)**	**Ethanol (%)**	**Wet Yield (g/L)**	**Dry Yield (g/L)**	**WHC (g/g)**
2	1	2.0270	1.4054	0.4054	512.36	3.54	143.65
17	2	0	2	1	466.90	3.78	122.42
11	3	7.9730	1.4054	1.5946	632.24	5.54	113.18
13	4	2.0270	2.5946	1.5946	550.64	4.77	114.41
32	5	5	2	1	570.60	4.32	131.08
1	6	2.0270	1.4054	0.4054	500.34	3.68	135.15

Table 4.3 The data of wet yield, dry yield, and water holding capacity from the laboratory experiment (Continued)

STD	Run	Factors			Responses		
		Sucrose* (%)	Tea (%)	Ethanol (%)	Wet Yield (g/L)	Dry Yield (g/L)	WHC (g/g)
34	7	5	2	1	597.70	4.63	128.06
21	8	5	1	1	619.05	4.58	134.05
20	9	10	2	1	350.63	3.33	104.29
16	10	7.9730	2.5946	1.5946	594.61	5.37	109.79
22	11	5	1	1	636.29	4.75	133.04
27	12	5	2	2	675.54	5.52	121.45
7	13	7.9730	2.5946	0.4054	612.56	5.94	102.07
24	14	5	3	1	552.14	4.51	121.45
30	15	5	2	1	589.35	4.67	125.17
12	16	7.9730	1.4054	1.5946	679.74	5.87	114.84
3	17	7.9730	1.4054	0.4054	667.51	3.54	143.65
29	18	5	2	1	586.55	4.61	126.23
25	19	5	2	0	372.12	3.38	109.03
26	20	5	2	0	417.43	4.43	93.25
8	21	7.9730	2.5946	0.4054	576.29	5.72	99.84
23	22	5	3	1	529.82	4.36	120.46
15	23	7.9730	2.5946	1.5946	561.57	5.32	104.62
28	24	5	2	2	627.10	5.75	107.99
19	25	10	2	1	426.18	3.74	112.92
9	26	2.0270	1.4054	1.5946	609.09	5.22	115.66
18	27	0	2	1	476.86	3.69	128.23
6	28	2.0270	2.5946	0.4054	551.06	3.94	138.83
10	29	2.0270	1.4054	1.5946	588.62	5.23	111.46

Table 4.3 The data of wet yield, dry yield, and water holding capacity from the laboratory experiment (Continued)

STD	Run	Factors			Responses		
		Sucrose* (%)	Tea (%)	Ethanol (%)	Wet Yield (g/L)	Dry Yield (g/L)	WHC (g/g)
33	30	5	2	1	642.82	5.03	126.85
31	31	5	2	1	561.20	4.36	127.69
14	32	2.0270	2.5946	1.5946	587.45	4.84	120.30
4	33	7.9730	1.4054	0.4054	668.37	4.92	134.82
5	34	2.0270	2.5946	0.4054	478.60	3.70	128.53

** Glucose was added to the sucrose until total weight of carbon source is 10%*

In this study, predicted values are not presented in the initial results table to maintain clarity and emphasize the actual experimental data used for model development. Predicted values are instead reported during the model validation stage, where they are compared with experimental results to assess the accuracy and reliability of the optimized conditions.

After inputting and analyzing the data, the software generated a summary of the response data, which is presented in **Table 4.4.**

Table 4.4 Summary of data analysis from the laboratory experiment

Res.	Obs.	Analysis	Min.	Max.	Mean	Sd	Ratio	Trans	Model
Wet yield (g/L)	34	Polynomial	350.63	679.74	560.86	84.33	1.94	None	Quadratic
Dry yield (g/L)	34	Polynomial	3.33	5.943	4.64	0.754	1.78	None	Quadratic
WHC (g/g)	34	Polynomial	93.25	143.65	120.64	12.56	1.54	None	Quadratic

Res. = Response, Obs. (Observation), Min. (Minimum), Max. (maximum), Sd (Standard deviation), Trans. (transformation), unit of WHC g/g (g water/g cellulose).

Table 4.4 provides detailed information about the response values, including minimum, maximum, mean, standard deviation (SD), transformation (Trans), ratio, and model. The wet yield from the experiments ranged from 350.63 g/L to 679.74 g/L, with a mean of 560.86 g/L and a SD of 84.33. The dry yield varied between 3.33 g/L and 5.943 g/L, with a mean of 4.64 g/L and a standard deviation of 0.754. The ratio of wet yield to dry yield was 1.94, reflecting the water content in the BC, which is critical for assessing its water retention capabilities. For WHC, the values ranged from 93.25 g/g to 143.65 g/g, with a mean of 120.64 g/g and a standard deviation of 12.56. The ratio for WHC was 1.54. The models developed in this study were quadratic polynomial models for all responses, as indicated in the table.

The 'Transform column in **Table 4.4** indicates whether a data transformation was applied during the analysis. For all responses (wet yield, dry yield, and WHC), the entry 'None' signifies that no transformations were needed. This suggests that the raw data met the assumptions required for statistical analysis and model development without the need for adjustments such as logarithmic or square root transformations. The quadratic polynomial models developed in this study establish a mathematical relationship between the independent variables and the responses, providing insights into how variations in the medium composition influence BC production. These models were found to be statistically significant and were validated through ANOVA.

4.4.2 Response Surface Analysis

The next phase of this study involved analyzing the data based on response parameters obtained from laboratory experiments. A software program was used to generate a comprehensive data analysis report, including transformations, fit summaries, model evaluations, ANOVA diagnostics, and graphical representations of the model.

1) Wet Yield Analysis

The Fit Summary for the quadratic model in the wet yield response demonstrates its suitability for predicting outcomes (**Table 4.5**). The model was chosen based on prior research suggesting a nonlinear relationship between the variables, where effects may change direction at a certain point, such as reaching an optimal threshold before decreasing. The model explains 54.76% of the variance (R^2), with an adjusted R^2 of 37.79%, indicating a moderate fit after accounting for the number of predictors. However, the predicted R^2 of 4.17% suggests that the model may not generalize well to new, unseen data, indicating potential overfitting. Additionally, the lack of fit value of < 0.0001 suggests that the model does not perfectly capture the underlying data patterns, with residuals significantly deviating from the observed values. This indicates that the quadratic model might not fully account for all the variability in the data. Despite these challenges, the quadratic model remains relevant due to its alignment with theoretical expectations of nonlinear effects and the possibility of an optimal threshold. The relatively low R^2, adjusted R^2, and predicted R^2 values are common in RSM studies involving biological systems like fermentation, where inherent variability and unmeasured factors contribute to response fluctuations.

The ANOVA results (**Table 4.6**) show that the overall model is significant for wet yield analysis (F-value = 3.23, p-value = 0.0105), meaning it explains a meaningful amount of variation in the response. Ethanol (C) has a significant effect on the response (p-value = 0.0042), while sucrose (A) and tea (B) do not (p-values of 0.3463 and 0.0793, respectively). The interactions between the factors and the quadratic effects of tea and ethanol are not significant. However, the quadratic effect of sucrose (A^2) is significant (p-value = 0.0092), suggesting a nonlinear relationship. The lack of fit is significant (F-value = 22.27, p-value < 0.0001), meaning the model does not fully capture the data, and there are differences between observed and predicted values. The addition information from the program is about the adequate precision (Adeq Precision). The adequate precision value of 5.9319 indicates the model has an

adequate signal for making predictions, although it may need refinement to better fit the data.

Table 4.5 The resume of fit summary report of wet yield analysis

Source	Sequential p-value	Lack of Fit p-value	R^2	Adjusted R^2	Predicted R^2	
Linear	0.0226	< 0.0001	0.2694	0.1963	0.035	
2FI	0.5614	< 0.0001	0.322	0.1713	-0.0307	
Quadratic	0.0194	< 0.0001	0.5476	0.378	0.0417	**Suggested**
Cubic	0.0071	< 0.0001	0.7689	0.6188	0.2399	**Aliased**

Table 4.6 ANOVA for Quadratic Model of wet yield analysis

Source	Sum of Squares	df	Mean Square	F-value	p-value	
Model	1.285E+05	9	14281.44	3.23	0.0105	significant
A-[Sucrose]	4082.45	1	4082.45	0.9228	0.3463	
B-[Tea]	14859.54	1	14859.54	3.36	0.0793	
C-[Ethanol]	44281.66	1	44281.66	10.01	0.0042	
AB	4230.79	1	4230.79	0.9563	0.3379	
AC	7656.69	1	7656.69	1.73	0.2007	
BC	455.33	1	455.33	0.1029	0.7511	
A^2	35524.13	1	35524.13	8.03	0.0092	
B^2	4951.52	1	4951.52	1.12	0.3006	
C^2	1056.54	1	1056.54	0.2388	0.6295	
Residual	1.062E+05	24	4423.97			
Lack of Fit	90701.46	5	18140.29	22.27	< 0.0001	significant
Pure Error	15473.81	19	814.41			
Cor Total	2.347E+05	33				

To predict the wet yield, the program generated a table displaying the final actual equation, which is presented as the Equation **(Eq.4.1)**. In this equation, S represents sucrose, T represents tea, and E represents ethanol. It is important to note that glucose must be added to ensure the total carbon source combination reaches 10% (w/v) of the total formulation. The effects of the interactions among sucrose, tea, and ethanol on the wet yield are illustrated in **Figure 4.1**, highlighting the influence of nutritional and additive compositions on the results of the wet yield.

$$Wet\ yield = 428.512 + 79.792[S] - 145.806[T] + 198.491[E] - 9.199[S][T] - 12.375[S][E] - 15.087[T][E] - 4.491[S]^2 + 41.915[T]^2 - 19.362[E]^2 \quad \textbf{(Eq. 4.1)}$$

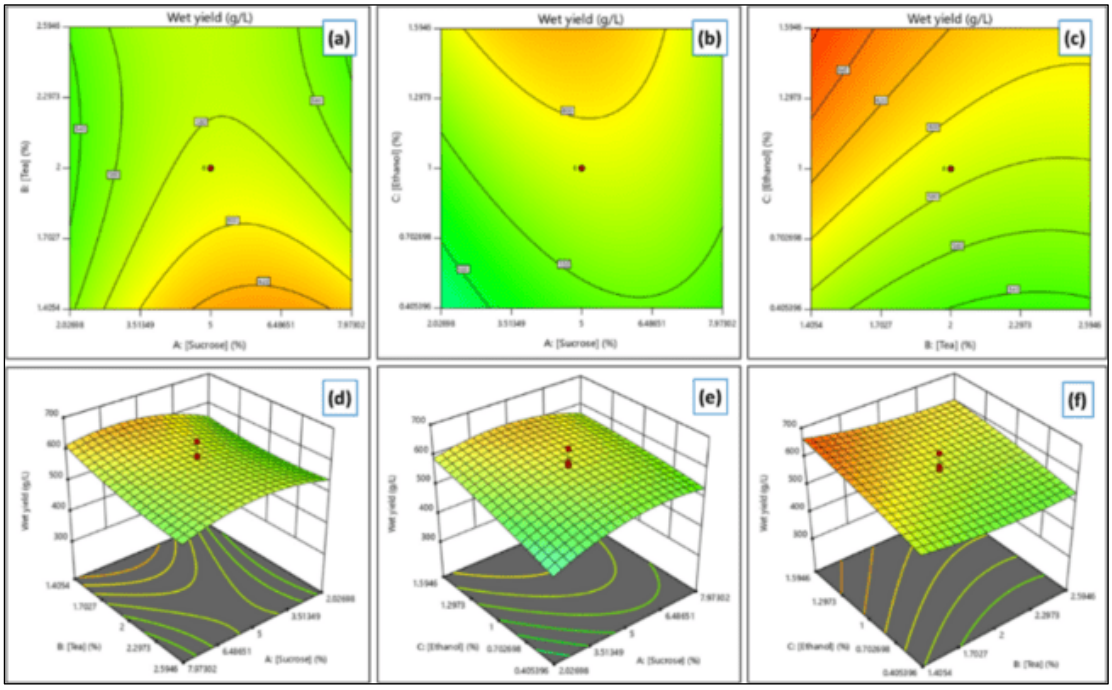

Figure 4.1 Graph model of the effect of formula composition interaction to the wet yield of BC.

The figure illustrates that the wet yield of BC increased due to specific interactions between the variables. An interaction between sucrose and tea concentrations showed an increase in BC yield, reaching its peak at a sucrose concentration of approximately 6.49% and a tea concentration of 1.41%. However, at

higher sucrose concentrations, around 7.97%, the yield began to decline (**Figure 4.1(a) and 4.1(d)**). Similarly, the interaction between sucrose and ethanol concentrations (**Figure 4.1(b) and 4.1(e)**) resulted in the highest BC productivity at a sucrose concentration of approximately 5% and an ethanol concentration of 1.59%. Additionally, the interaction between tea and ethanol concentrations (**Figure 4.1(c) and 4.1(f)**) contributed to an increase in BC yield, with the maximum productivity observed at a tea concentration of 1.41% and an ethanol concentration of 1.59%.

2) Dry Yield Analysis

The Fit Summary for the quadratic model in the dry yield response underscores its potential suitability for predicting outcomes (**Table 4.7**). This model was chosen based on evidence suggesting that the relationship between variables may be nonlinear, with effects reaching a maximum point before declining. The model explains 67.71% of the variance (R^2) and the adjusted R^2 of 55.61% indicates a moderate level of explanatory power after accounting for the number of predictors. The predicted R^2 of 0.3217 suggests the model has reasonable predictive ability for new data, though it may still have limitations in generalization. However, the significant lack of fit ($p < 0.0001$) indicates that the model does not fully capture the complexity of the data, as the residuals deviate considerably from the observed values. Despite these shortcomings, the quadratic model remains relevant, as it aligns with the theoretical expectations of nonlinear relationships and provides valuable insights into the interactions between variables affecting dry yield.

Table 4.7 The resume of fit summary report of dry yield analysis

Source	Sequential p-value	Lack of Fit p-value	R^2	Adjusted R^2	Predicted R^2	
Linear	0.0017	< 0.0001	0.3919	0.3311	0.1909	
2FI	0.0885	< 0.0001	0.5205	0.4139	0.2565	
Quadratic	0.0215	< 0.0001	0.6771	0.5561	0.3217	**Suggested**
Cubic	0.0166	< 0.0001	0.819	0.7013	0.4166	**Aliased**

The ANOVA results (**Table 4.8**) demonstrate that the overall quadratic model is significant for dry yield analysis, with an F-value of 5.59 and a p-value of 0.0003. This indicates that the model explains a substantial portion of the variation in the response. Among the individual factors, sucrose (A) and ethanol (C) significantly impact the dry yield, with p-values of 0.0068 and 0.0001, respectively. However, tea (B) does not have a significant effect, as indicated by its p-value of 0.9656. For interaction effects, none of the interactions between factors (AB, AC, BC) show a significant influence on dry yield, as their p-values exceed the 0.05 threshold. Additionally, the quadratic terms (A^2), (B^2), and (C^2) show varying levels of influence but do not meet the criteria for statistical significance, with p-values of 0.0578, 0.2974, and 0.0844, respectively.

Table 4.8 ANOVA for Quadratic Model of dry yield analysis

Source	Sum of Squares	df	Mean Square	F-value	p-value	
Model	12.69	9	1.41	5.59	0.0003	significant
A-[Sucrose]	2.21	1	2.21	8.78	0.0068	
B-[Tea]	0.0005	1	0.0005	0.0019	0.9656	
C-[Ethanol]	5.13	1	5.13	20.35	0.0001	
AB	0.1875	1	0.1875	0.7435	0.3971	
AC	1.22	1	1.22	4.82	0.0380	
BC	1.01	1	1.01	3.99	0.0572	
A^2	1.00	1	1.00	3.97	0.0578	
B^2	0.2860	1	0.2860	1.13	0.2974	
C^2	0.8175	1	0.8175	3.24	0.0844	
Residual	6.05	24	0.2522			
Lack of Fit	4.89	5	0.9782	16.01	< 0.0001	significant
Pure Error	1.16	19	0.0611			
Cor Total	18.74	33				

The lack of fit is significant, with an F-value of 16.01 and a p-value of less than 0.0001, suggesting that the model does not fully capture the complexity of the data. This indicates discrepancies between observed and predicted values, pointing to areas where the model could be refined for improved accuracy. Additionally, the model's adequate precision value of 8.6008 exceeds the recommended minimum threshold of 4.0, indicating that the model has a sufficient signal-to-noise ratio for making reliable predictions. While adequate precision suggests the model's predictions are reasonable, the significant lack of fit highlights the need for further refinement to better align the model with the observed data.

To estimate the dry yield, the program provided a table with the final actual equation, which is reformulated and shown as Equation 4.2 (**Eq. 4.2**). In this equation, S, T, and E represent sucrose, tea, and ethanol, respectively. Additionally, glucose must be incorporated to ensure the total carbon source combination equals 10% (w/v) of the overall formulation. **Figure 4.9** illustrates the impact of interactions between sucrose, tea, and ethanol on the dry yield, emphasizing the role of nutritional and additive compositions in influencing the results.

$$Dry\ yield = 2.975 + 0.368[S] - 0.864[T] + 1.850[E] + 0.061[S][T] - 0.156[S][E] - 0.709[T][E] - 0.024[S]^2 + 0.319[T]^2 + 0.539[E]^2$$

.....(**Eq. 4.2**)

The figure demonstrates that the dry yield of BC is influenced by interactions between the variables. The interaction between sucrose and tea concentrations led to an increase in BC dry yield, peaking at a sucrose concentration of approximately 7.97% and a tea concentration of about 2.59% (**Figure 4.2(a) and 4.2(d)**). The interaction between sucrose and ethanol concentrations resulted in the highest dry yield at a sucrose concentration of approximately 5.00% and an ethanol concentration of 1.59% (**Figure 4.2(b) and 4.2(e)**). Furthermore, the interaction between tea and ethanol concentrations contributed to an enhanced BC yield, with

maximum productivity observed at a tea concentration of 1.41% and an ethanol concentration of 1.59% (**Figure 4.2(c) and 4.2(f)**).

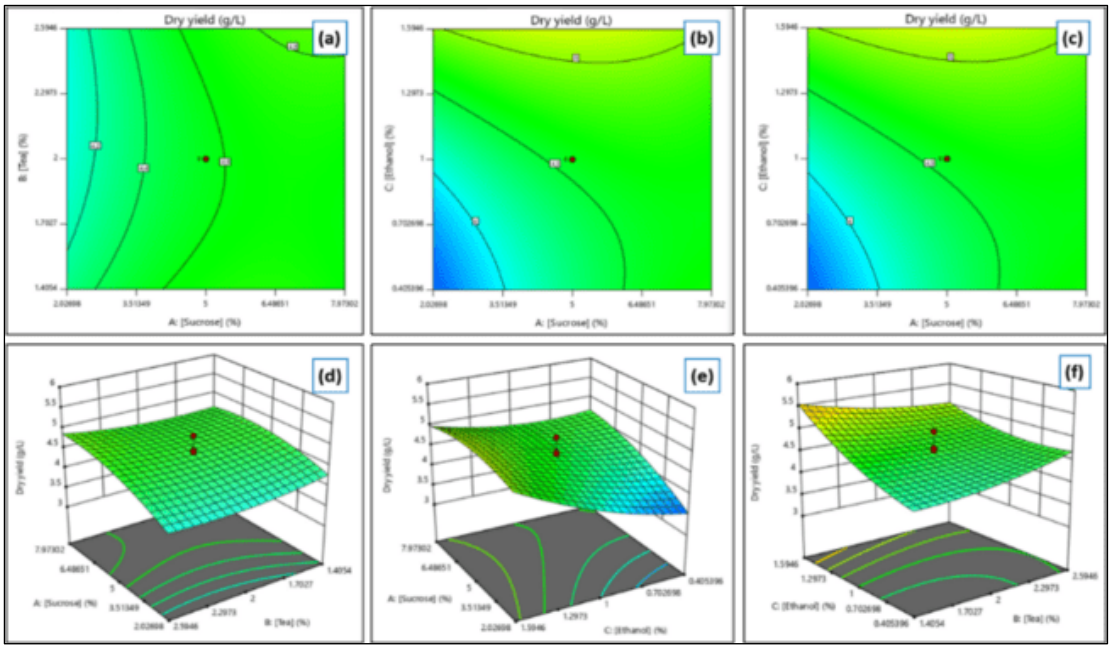

Figure 4.2 Graph model of the effect of formula composition interaction to the dry yield of BC.

3) Water Holding Capacity (WHC) Analysis

The Fit Summary for the quadratic model in the WHC response highlights its potential suitability for understanding the interactions among variables (**Table 4.9**). This model was selected as it aligns with theoretical expectations of nonlinear relationships, where effects may increase to a maximum point before declining. The model explains 70.4% of the variance (R^2), while the adjusted R^2 of 59.3% reflects a moderate explanatory power after accounting for the number of predictors. The predicted R^2 of 0.3665 suggests the model has reasonable predictive ability for new data, though its generalization may still be limited. However, the significant lack of fit ($p = 0.0001$) indicates that the model does not fully capture the complexity of the data, as residuals deviate substantially from observed values. Despite these limitations, the quadratic model provides valuable insights into the

nonlinear interactions influencing WHC and remains a relevant tool for exploring variable relationships.

Table 4.9 The resume of fit summary report of dry yield analysis

Source	Sequential p-value	Lack of Fit p-value	R^2	Adjusted R^2	Predicted R^2	
Linear	0.0101	< 0.0001	0.3102	0.2412	0.0921	
2FI	0.0328	< 0.0001	0.4983	0.3868	0.2421	
Quadratic	0.0048	0.0001	0.704	0.593	0.3665	Suggested
Cubic	0.0002	0.0655	0.8981	0.8318	0.6588	Aliased

The ANOVA results (**Table 4.10**) confirm that the quadratic model is significant for the analysis of WHC, with an F-value of 6.34 and a p-value of 0.0001. These results indicate that the model accounts for a substantial portion of the variability in WHC. Among the individual factors, sucrose (A) and tea (B) have significant effects on WHC, with p-values of 0.0021 and 0.0039, respectively. In contrast, ethanol (C) does not exhibit a statistically significant effect, as indicated by its p-value of 0.0907.

Significant interactions are also observed. The interaction between sucrose and tea (AB) is notable, with a p-value of 0.0155, as is the interaction between tea and ethanol, with a p-value of 0.0210. Additionally, the quadratic effect of ethanol (C^2) is significant, with a p-value of 0.0014, suggesting the presence of a nonlinear relationship between ethanol concentration and WHC. These findings underscore the importance of considering both individual factors and their interactions when evaluating WHC.

The lack of fit is significant (F-value = 9.45, p-value = 0.0001), indicating that the model does not fully capture the complexity of the data and that discrepancies exist between the observed and predicted values. However, the adequate precision value of 9.040 exceeds the recommended threshold of 4.0,

indicating that the model has a sufficient signal-to-noise ratio and is reliable for predictive purposes. While the significant lack of fit suggests room for improvement, the model's overall performance justifies its continued use. The model provides valuable insights into the factors influencing WHC and offers a reliable foundation for further refinement and optimization.

Table 4.10 ANOVA for Quadratic Model of WHC

Source	Sum of Squares	df	Mean Square	F-value	p-value	
Model	3662.98	9	407.00	6.34	0.0001	significant
A-[Sucrose]	761.53	1	761.53	11.87	0.0021	
B-[Tea]	653.03	1	653.03	10.18	0.0039	
C-[Ethanol]	199.39	1	199.39	3.11	0.0907	
AB	435.91	1	435.91	6.79	0.0155	
AC	151.15	1	151.15	2.36	0.1379	
BC	391.75	1	391.75	6.10	0.0210	
A^2	189.73	1	189.73	2.96	0.0984	
B^2	12.19	1	12.19	0.1900	0.6669	
C^2	837.94	1	837.94	13.06	0.0014	
Residual	1540.18	24	64.17			
Lack of Fit	1098.58	5	219.72	9.45	0.0001	significant
Pure Error	441.60	19	23.24			
Cor Total	5203.16	33				

The program generated a table with the final actual equation for estimating WHC, which has been reformulated and presented as Equation 7.3. (**Eq. 4.3**) In this equation, S, T, and E correspond to sucrose, tea, and ethanol, respectively. Furthermore, glucose is included to ensure that the total carbon source combination reaches 10% (w/v) in the overall formulation. **Figure 4.3** highlights the interactions

between sucrose, tea, and ethanol on WHC, showcasing the influence of both nutritional and additive compositions on the observed outcomes.

$$WHC = 147.174 + 5.673[S] - 15.775[T] - 6.743[E] - 2.953[S][T] + 1.739[S][E] + 13.996[T][E] - 0.328[S]^2 + 2.080[T]^2 - 17.243[E]^2 \quad \text{(Eq. 7.3)}$$

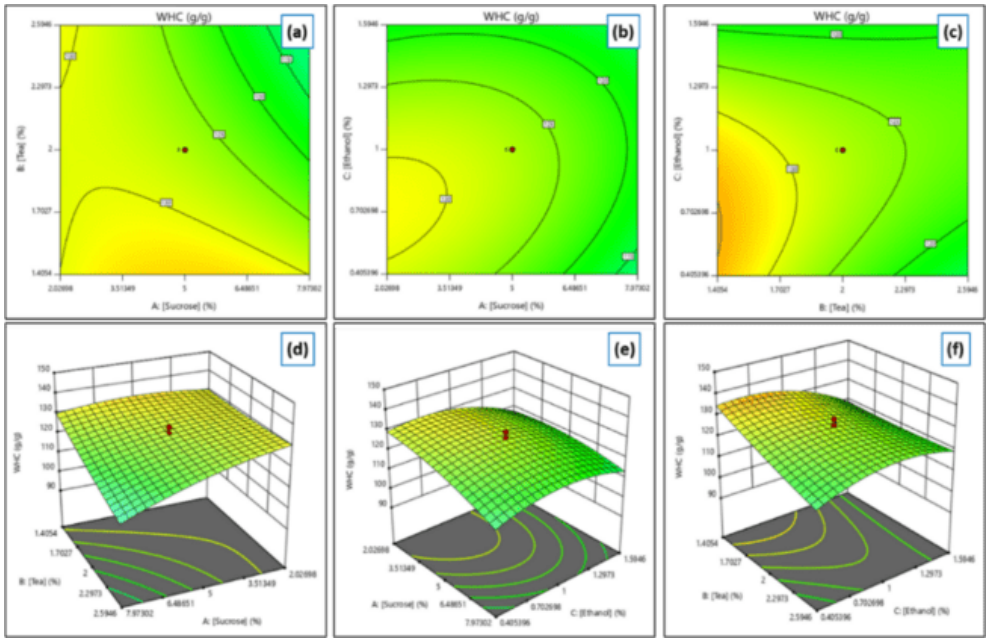

Figure 4.3 Graph model of the effect of formula composition interaction to WHC of BC.

The **Figure 4.3** demonstrates that the WHC of BC is influenced by interactions between the variables or factors. The interaction between sucrose and tea concentrations led to an increase in WHC, peaking at a sucrose concentration of approximately 5.00% and a tea concentration of about 1.41% (**Figure 4.3(a) and 4.3(d)**). Similarly, the interaction between sucrose and ethanol concentrations resulted in the highest WHC at a sucrose concentration of approximately 5.00% and an ethanol concentration of 1.59% (**Figure 4.3(b) and 4.3(e)**). Furthermore, the interaction between tea and ethanol concentrations contributed to an enhanced BC yield, with maximum productivity observed at a tea concentration of 1.41% and an ethanol concentration of 1.59% (**Figure 4.3(c) and 4.3(f)**).

4.4.3 Optimization of Formula, Validation, and Data Confirmation

The formula optimization was performed using the software by establishing specific criteria for the process. The primary objective was to maximize the wet yield of BC production, with the assumption that the dry yield would correlate closely with the wet yield due to the WHC values remaining within the specified range. The goal is to achieve the highest yield while utilizing raw materials economically and efficiently. The summary of the criteria setting and its constraints are presented in **Table 4.11**. The optimization process results (generated by the software) were presented in a Table containing multiple alternative medium formulations (**See Appendix C, Table 6.).** Among these, one formula was highlighted as the most optimal, featuring the highest desirability value (close to 1). The software generated approximately 53 formulations. From these, three sample formulas were selected for experimental testing: the most frequently recommended by the program (RTC-V1), the formulation with the highest predicted yield (RTC-V46), and the one with the lowest predicted yield (RTC-V53). These codes (RTC-V1, RTC-V46, RTC-V53) serve as identifiers for the experiments to facilitate easier reference. The letter "V" denotes the validation step, and the number following it indicates the solution or formula order. Details of the selected formulations and their predicted responses are presented in **Table 4.12**.

The selected formula was validated through laboratory experiments, and the experimental results were used to confirm the predictions provided by the software. The confirmation data is presented in **Table 4.13**, demonstrating that the experimental outcomes align well with the predicted values. These findings validate the accuracy of the equation and the selected formula for BC production. Notably, the most recommended formula achieved a wet yield of 621.71 g/L, representing a 238.54% increase compared to the highest yield obtained in the preliminary study (RTC-SGlu), discussed in an earlier chapter of this thesis. Similarly, the dry yield increased by 214.67%, while the WHC results were comparable to the previous findings.

Table 4.11 Summary of the criteria and constraints for optimizing the medium formulation.

Name	Goal	Lower Limit	Upper Limit	Lower Weight	Upper Weight	Importance
A: [Sucrose]	maximize	2.027	7.973	1	1	5
B: [Tea]	minimize	1.405	2.594	1	1	3
C: [Ethanol]	is in range	0.405	1.594	1	1	3
Wet yield	maximize	350.62	679.74	1	1	5
Dry yield	is in range	3.33	5.94	1	1	3
WHC	is in range	93.25	143.65	1	1	3

Glucose was added to the sucrose solution to reach a final concentration of 10%. The lower and upper limits for the optimization variables were automatically determined by the software based on prior experimental data from laboratory experiment.

Table 4.12 Software-Generated Optimal Formula and Predicted BC Production

No/Code	Sucrose	Tea	Ethanol	Wet yield	Dry yield	WHC	Desira-bility
RTC-V1	7.973	1.405	1.595	630.159	5.238	119.265	0.939
RTC-V46	7.260	1.407	1.595	645.117	5.35	119.754	0.912
RTC-V53	7.973	1.405	0.580	593.081	4.446	130.125	0.889

Codes (RTC-V1, RTC-V46, RTC-V53) identify experiments; "V" indicates the validation step, and the number represents the solution order of the selected formula

RSM has been widely recognized as an effective tool for optimizing BC production. This study successfully increased BC productivity, aligning with previous research that demonstrated the efficacy of RSM in enhancing BC yields. Approaches such as CCD and Rotatable CCD have consistently resulted in significant improvements in BC productivity under optimized conditions (Hegde et al. 2013; Singh et al. 2017; Rodrigues et al. 2019; Aswini et al. 2020; Yilmaz and Goksungur 2024).

Table 4.13 Software-Generated Data Confirmation Output

Sample Code	Response	Predicted Mean	n	95% PI low	Actual Mean	95% PI high
	Wet yield	630.16±54.37	3	517.94	621.71±24.06	742.37
RTC-V1	Dry yield	5.24±0.41	3	4.39	5.56±0.50	6.09
	WHC	119.27±6.55	3	105.75	107.32±8.01	132.78
	Wet yield	645.12±51.31	3	539.22	658.66±34.91	751.02
RTC-V46	Dry yield	5.35±0.39	3	4.55	5.56±0.33	6.15
	WHC	119.77±6.18	3	107.02	115.08±8.81	132.53
	Wet yield	593.19±50.85	3	488.16	593.88±39.27	698.06
RTC-V53	Dry yield	4.45±0.38	3	3.65	5.09±0.92	5.24
	WHC	130.13±6.12	3	117.49	115.60±17.24	142.77

Two-sided Confidence = 95%, n = the number of replications. Unit for yield (g/L) and unit for WHC (g water/ g cellulose)

4.4.4 Characterization of BC Product Resulted from Selected Formula

1) BC productivity and water holding capacity

BC produced from kombucha fermentation with different composition of the medium formulation on the wet yields, dry yields, and WHC, as shown in **Figure 4.4**. The results showed that different formulation that was suggested by the program i.e. RTC-V1, RTC-V46, and RTC-V53 are not significantly different ($P > 0.05$) in the wet yield ($P = 0.135$), dry yield ($P = 0.377$), and water holding capacity ($P = 0.544$).

RSM has been used to optimize BC production. In earlier studies, the CCD, a form of RSM, was applied to optimize BC production, resulting in a sixfold increase (0.318% to 1.72% (w/v)) in BC productivity (Hegde et al. 2013). Using the Rotatable Central Composite Design (RCCD), RSM successfully increased BC production by optimizing five independent variables—temperature, pH, incubation time, molasses concentration, and corn steep liquor concentration—each at five levels, achieving a

maximum yield of 4.34 g/L (dry weight), compared to a regular yield of approximately 3.85 g/L after 172 hours of fermentation (Singh et al. 2017). CCD has also been reported to significantly enhance BC productivity (Rodrigues et al. 2019). Optimization using RSM under optimal conditions yielded the highest BC productivity of approximately 469.83 g/L (wet weight) (Aswini et al. 2020). An RSM-based study further enhanced BC productivity, achieving a fivefold increase compared to the regular medium, reaching 8.45 g/L (dry weight) (Yilmaz and Goksungur 2024). The WHC of BC observed in this study is comparable to or within the range of results reported in the previous chapter.

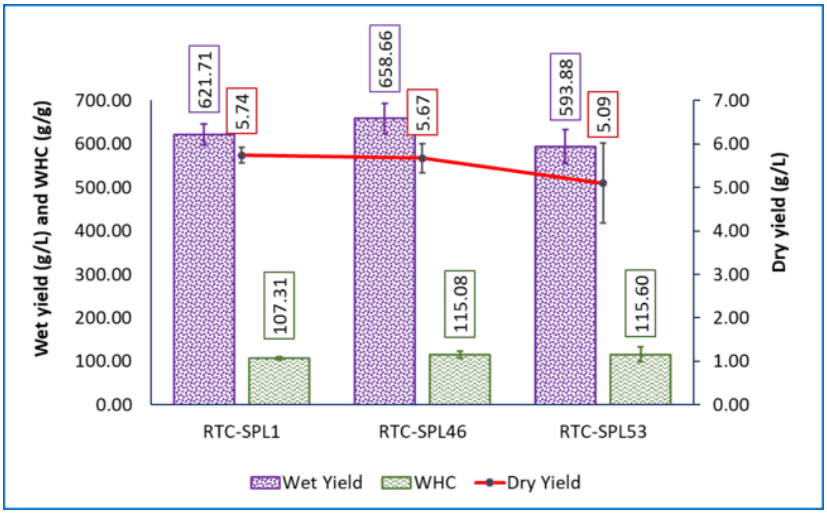

Figure 4.4 Wet yield (g/L), Dry yield (g/L), and WHC (g water/g cellulose) of purified BC from kombucha fermentation with different type of tea.

2) Morphology Analysis (SEM)

The morphology of BC samples produced from kombucha fermentation using various medium formulations—RTC-V1, RTC-V46, and RTC-V53—was examined through scanning electron microscopy (SEM). Each sample was observed at magnifications of 10,000x, 30,000x, and 50,000x (**Figure 4.5**). The fiber diameter distribution of dried BC was analyzed using the ImageJ software, and the results are presented in **Figure 4.6**. For comparison, RTC-C was included in this analysis. Overall, the SEM images revealed similar morphologies among the samples, displaying a uniform fiber pattern consistent with findings from previous studies.(Illa et al. 2019;

Brandes et al. 2020; Nguyen and Nguyen 2022). However, the BC fiber size appeared larger after optimization compared to the RTC control, likely due to differences in medium composition. This observation is supported by the fiber diameter analysis, which showed that the fiber diameters of RTC-V1, RTC-V46, and RTC-V53 were 37.85 ± 6.46 nm, 38.42 ± 7.52 nm, and 38.87 ± 6.91 nm, respectively, significantly larger than the RTC-C control, which had a fiber diameter of 30.65 ± 6.46 nm. In a previous chapter, BC produced using a medium containing a combination of sucrose and glucose (RTC-SGlu) had a fiber diameter of 34.33 ± 7.56 nm, while BC produced with ethanol as an additive (RTC-EtOH) exhibited a fiber diameter of 45.98 ± 9.38 nm.

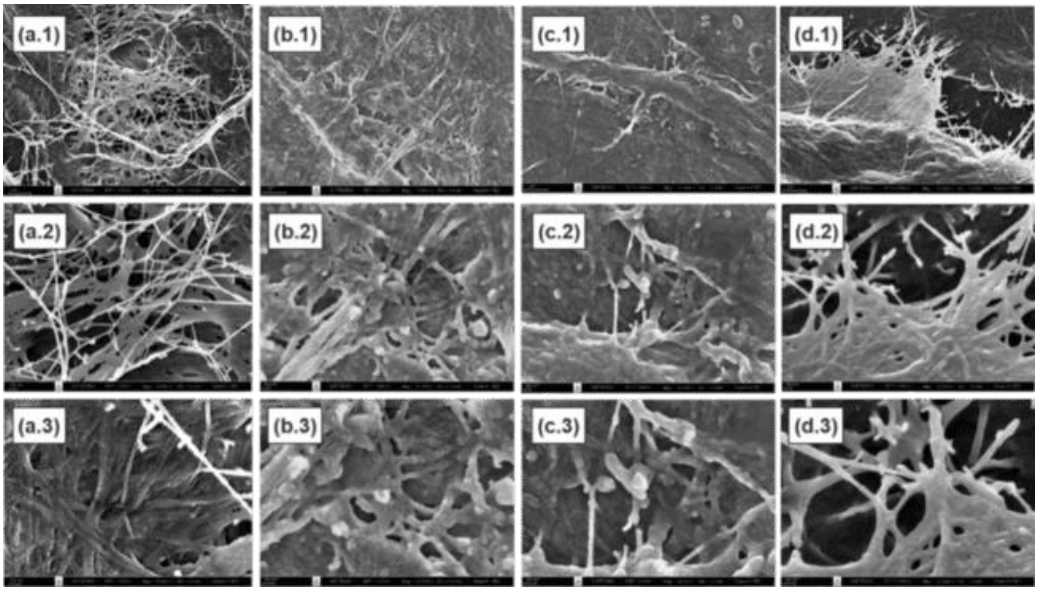

Figure 4.5 SEM image of BC from (a) RTC-C, (b) RTC-V1, (c) RTC-V46, and (d) RTC-V53. (1) 10k, (2) 30k, and (3) 50k magnifications.

The results of this study align with previous findings on BC fiber diameters. *K. hansenii* 23769 (ATCC) and a strain isolated from grape juice (GBHS) produced BC fibers with average diameters of 28.9 ± 5.6 nm and 28.6 ± 6.7 nm, respectively (Illa et al. 2019). Similarly, *K. rhaeticus* PG2 cultivated in HS medium using glucose and glycerol as carbon sources produced BC fibers with diameters of 30–60 nm (Thorat and Dastager 2018). BC nanofibers derived from HS medium and waste fig medium had average diameters of 36 nm and 44 nm, respectively (Yilmaz and

Goksungur 2024). In low-cost media like date syrup and cheese whey, *K. xylinus* produced fibers averaging 45–55 nm (Raiszadeh-Jahromi et al. 2020). Wang et al. (2018) also reported BCNFs with diameters of 35–50 nm using various carbon sources (Wang et al. 2018).. In contrast, glucose supplemented with 1.5% ethanol resulted in larger fiber diameters of 64.1 ± 5.11 nm to 82.3 ± 3.28 nm, which increased further with 3% ethanol (Fatima et al. 2023). These findings highlight the influence of carbon source composition and ethanol supplementation in the optimized formulation on BC fiber morphology.

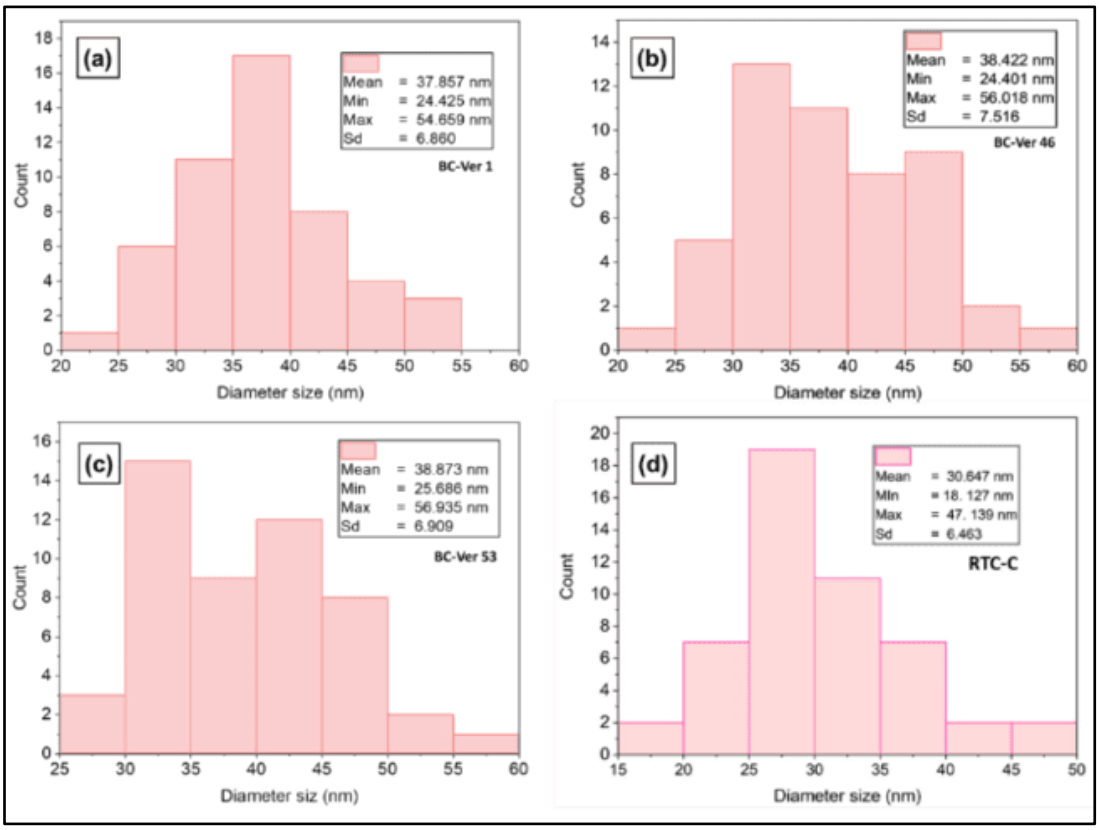

Figure 4.6 Graph of the polydispersity in fiber diameter for BC samples: (a) RTC-V1, (b) RTC-V46, (c) RTC-V53, and (d) RTC-C.

3) Fourier Transform Infrared Spectroscopy Analysis

Figure 4.7 shows the FTIR spectra of BC samples produced from various optimized medium kombucha fermentation with i.e. RTC-V1, RTC-V46, and RTC-V53. RTC-C is used for comparison. The FTIR spectra of the BC samples reveal distinct

differences, particularly in the optimized samples compared to RTC-C. These differences highlight the impact of adding glucose and ethanol to the medium, in addition to sucrose and Thai red tea solution used in the control sample (RTC-C).

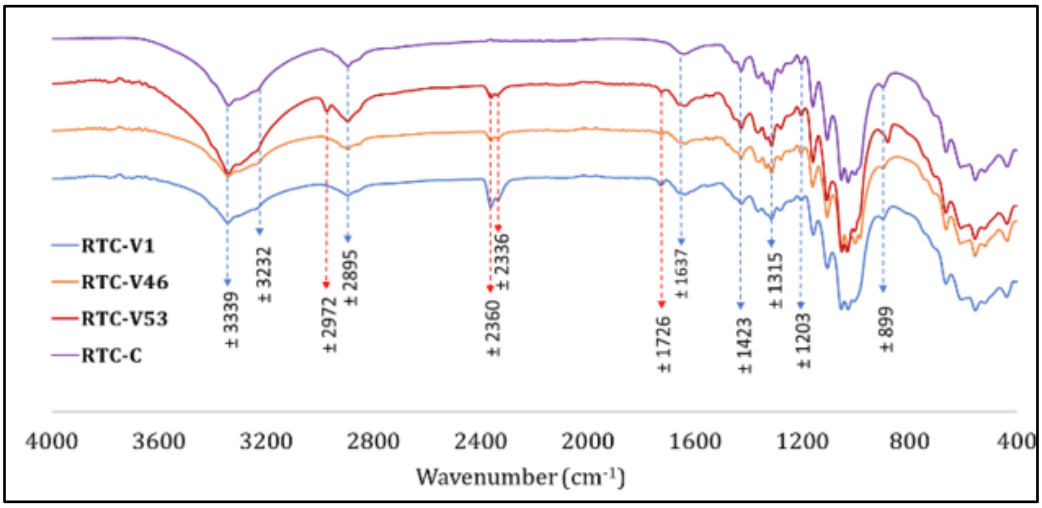

Figure 4.7 FTIR spectra of BCs from various of medium formulations i.e. RTC-V1, RTC-V46, RTC-V53, and RTC-C.

Some keys observation is the appearance of a band at 2972 cm^{-1} (particularly in RTC-V53) and then peak at around 2360 cm^{-1}, 2336 cm^{-1}, and 1726 cm^{-1}. The peaks observed at approximately 3339 cm^{-1} and 3232 cm^{-1} correspond to O-H stretching vibrations, which are characteristic of hydroxyl groups. The subtle differences in peak intensity suggest variations in the hydrogen bonding network among the samples. Additionally, the peak around 2895 cm^{-1} is attributed to C-H stretching vibrations, which are typically associated with aliphatic groups such as CH2 or CH3 (Leonarski et al. 2021a; Fatima et al. 2023).

The peak observed at 2972 cm^{-1} (in RTC-V53) is likely due to the stretching vibrations of C-H bonds in methyl and methylene groups, which may result from the addition of ethanol to the fermentation medium. However, this band is absent or less pronounced in the control sample (RTC-C) and the other optimized samples (RTC-V1, RTC-V46). The faint peaks observed around 2360 cm^{-1} and 2336 cm^{-1} in optimized BCs suggests the presence of triple-bond functional groups, such as C≡C

or C≡N (Srivastava and Mathur 2022). These groups could originate from polyphenols and other organic compounds, protein, yeast cell, and bacteria (Amarasekara et al. 2020). The same observation was reported in previous studies, such as BC derived from *nata de coco* (Fuller et al. 2018; Rachtanapun et al. 2021). Fuller et al. (2018) noted that this peak was present in samples contaminated with residual proteins, nucleic acids, and whole cells (Fuller et al. 2018). The incorporation of these impurities into the BC matrix may be attributed to the thick and dense structure of the pellicle, which can hinder complete removal during the purification process. Evidence of such impurities can also be seen in the SEM images (**Figure 4.5**).

The peak around 1726 cm^{-1} in purified BC is likely attributed to the C=O stretching vibration of carbonyl groups, which are commonly found in aldehyde groups (1720–1740 cm^{-1}), ketones (1705–1725 cm^{-1}), and carboxylic acids (1700–1725 cm^{-1}) (Yao et al. 2015). These groups may originate from polyphenols and other organic compounds, as well as proteins, yeast cells, and bacterial components (Amarasekara et al. 2020). Fuller et al. (2018) reported that the presence of impurities contributes to the emergence of bands between 1800 cm^{-1} and 1500 cm^{-1}, which are attributed to functional groups such as NH_2, C–N, and C=O, originating from lipids, proteins, and nucleic acids (Fuller et al. 2018).

4) X-Ray Diffraction (XRD) Analysis

The XRD analysis of BC samples, including optimized (RTC-V1, RTC-V46, RTC-V53) and control (RTC-C) formulations are demonstrated **Figure 4.8**. The Crystallinity index and the crystallite size of BC the optimized BC samples and control of BC from Thai red tea kombucha are presented in **Table 4.14**. The XRD spectra visualized the characteristics diffraction peaks at around 14.54°, subtle peak at around 17.11°, and 23.03° (2θ).

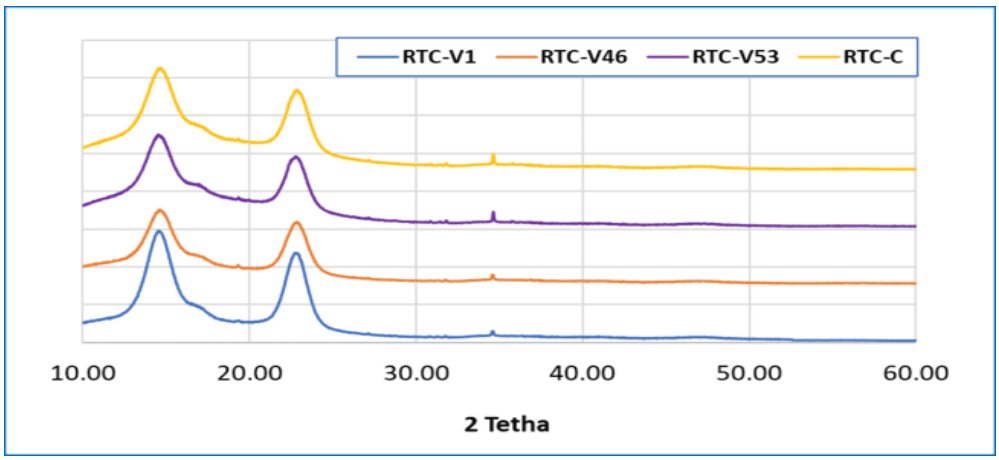

Figure 4.8 XRD spectra of BCs from various of medium formulations i.e. RTC-V1, RTC-V46, and RTC-V53.

The observed peaks confirm the crystalline structure characteristic of BC, consistent with previous findings reported by Said Azmi et al. (Said Azmi et al. 2023). The XRD profiles closely match those described in earlier studies on BC (Revin et al. 2018; Jittaut et al. 2023; Said Azmi et al. 2023), as well as the results presented in the previous chapter of this study. While the XRD patterns confirm the uniform chemical structure across the samples, variations in diffraction peak intensities are noticeable, suggesting subtle differences in the cellulose chain orientation (Said Azmi et al. 2023). The most prominent peak observed near 23° corresponds to the characteristic cellulose type I (Said Azmi et al. 2023; Hossen et al. 2024). According to Gaspar et al. peaks at 2θ values of 14.7°, 16.8°, and 22.7° can be attributed to the 100, 110, and 200 crystallographic planes, which are typical of native cellulose type I (Gaspar et al. 2014). Similarly, the peak appearing at approximately 22.90° (2θ) further confirms the crystalline nature of the cellulose samples (Samuel and Adefusika 2019). These results align with previous observations, reinforcing the consistency of BC's structural properties across various studies.

The CI and crystallite size of BC samples were calculated from the XRD data using the Segal method, which involves assessing the peak height and subtracting baseline intensity. As shown in **Table 4.14**, the results reveal slight

variations in peak intensities, indicating changes in crystallinity. The control sample (RTC-C) exhibits the highest crystallinity index (86.74%) with the most intense peaks, suggesting a more ordered cellulose structure. In comparison, the optimized samples display slightly reduced crystallinity, with RTC-V1, RTC-V46, and RTC-V53 showing values of 83.23%, 84.46%, and 85.97%, respectively. This reduction is likely due to the inclusion of ethanol and glucose in the fermentation medium, which may disrupt the alignment of cellulose chains during synthesis. This observation is consistent with findings from the previous chapter, where the use of a combination of sucrose and glucose as carbon sources, as well as ethanol as an additive, resulted in BC samples with lower crystallinity (around 86.00% and 80.22%, respectively).

Table 4.14 CI and crystallite size of BC samples from various of medium formulations i.e. RTC-V1, RTC-V46, and RTC-V53.

Parameter	RTC-C	RTC-V1	RTC-V46	RTC-V53
Crystallinity index (%)	89.54	83.23	84.46	85.97
Crystallite size (nm)	3.34	3.19	3.33	3.30

The CI results of this study are consistent with those reported in previous research. For instance, BC produced from pineapple peel waste fermentation achieved a CI of 87% (Sardjono et al. 2019), while BC derived from pineapple waste solution had a CI of 82.2% (Pham and Tran 2023). Similarly, BC obtained from citrus processing waste exhibited a CI of 86.9% (Andritsou et al. 2018). Heydorn et al. reported a CI range of 57% to 85% for BC produced in HS medium using various carbon sources (Heydorn et al. 2023). In addition, BC without interfering components demonstrated a CI of 84%–90%, as observed by (Cazón and Vázquez 2021). Slightly lower CI values were noted in BC produced from crude distillery effluent (80.2%) (Gayathri and Srinikethan 2019), and wastewater from Arenga starch production (79.6%) (Rahmayetty and Sulaiman 2023). These findings further validate the results presented in the previous chapter of this study.

Further analysis of the average crystallite size of BC (**Table 4.14**), which reflects the dimension of ordered crystalline regions, reveals minor variations among the samples. The control sample has the largest crystallite size (3.34 nm), while the optimized samples exhibit slightly smaller sizes: 3.19 nm for RTC-V1, 3.33 nm for RTC-V46, and 3.30 nm for RTC-V53. This reduction can be attributed to the altered fermentation medium, where ethanol and glucose may have influenced the biosynthetic process of cellulose, leading to finer crystalline structures.

Several of the previous studies reported the average of BC diameter size from the lower to the higher results. BC produced by *G. xylinus* InaCC B404 in HS medium has average crystallite size of 3.06 nm for BC produced by (Agustin et al. 2021). Average crystallite sizes of BC range from 3.29 nm and 4.80 nm were observed in BC produced from black tea kombucha after 3 and 5 days of fermentation, respectively (Balistreri et al. 2024). More results of the studies reported the higher average crystallite size such as BC derived from *K. xylinus* strains using fructose and glucose as carbon sources exhibited crystallite sizes ranging from 4.7 to 6.8 nm (Singhsa et al. 2018). BC produced by *Lactobacillus plantarum* in a green tea leaf solution (1% green tea, 10% sucrose) had crystallite sizes of 5.36, 5.94, and 5.98 nm after 7, 14, and 30 days of fermentation, respectively (Charoenrak et al. 2023). BC produced under different conditions also exhibited crystallite sizes of 5.6 nm (Jia et al. 2017) and 8.36 nm (Gayathri and Srinikethan 2019). These results highlight the impact of fermentation medium composition on the structural characteristics of BC. The crystallinity of BC can be influenced by several factors, including carbon and nitrogen sources, type of additives, bacterial strains, fermentation conditions such as temperature and duration, and the methods used in post-production processing (Zeng et al. 2011; Thielemans et al. 2023).

5) Thermogravimetric (TGA/DTG) Analysis

Figure 4.9 depicts the thermogravimetric (TG) and differential thermal degradation (DTG) curves for BC samples. The results were gathered using

thermogravimetric analysis (TGA). From the spectra graph, it is observed that overall optimized BC has similar spectra pattern. However, a slightly distinction is observed in the graph, particularly in DTG graph, optimized BC has lower DTG T_{Max} temperature compare to control (RTC-C). The analysis detail of TGA and TG analysis result is summarized in **Table 4.15**.

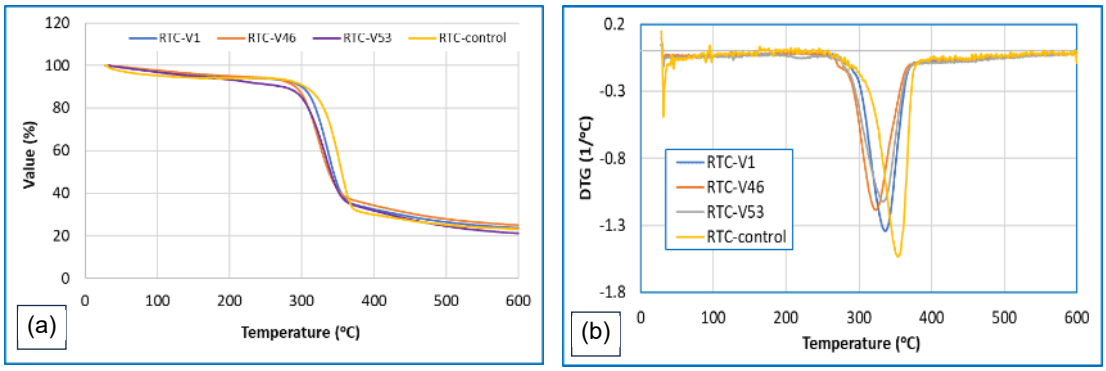

Figure 4.9 TGA (a) and DTG (b) thermograph of optimized and control BC samples

In the TGA analysis, the first-stage weight loss, ranging from 5.25% to 7.47%, is attributed to the dehydration and volatilization of low-molecular-weight components or residual water within the BC matrix (Teixeira et al. 2019; Mohamad et al. 2022a). RTC-V1 and RTC-V46 exhibited first-stage weight losses of 5.25% and 5.62%, respectively, which were slightly lower than that of RTC-C (6.03%). In contrast, RTC-V53 demonstrated a higher weight loss of 7.74%. This value exceeds the range reported by Gismatulina and Budaeva (1 – 2%) (Gismatulina and Budaeva 2024) but aligns closely with findings from Mohamad et al., who observed a weight loss of 5 – 9% (Mohamad et al. 2022a).

The second-stage weight loss, occurring between 240°C and 600°C across the samples, exhibited relatively consistent values ranging from 69.70% to 71.35%. The remaining material (residue) after decomposition at 600°C ranged from 21.14% to 25.02%. Compared to previous experiments, BC produced using RTC-SGlu and RTC-EtOH showed second-stage weight losses of 73.90% and 68.13% and residues of 20.92% and 28.52%, respectively. In earlier results, RTC-C demonstrated a higher

second-stage weight loss and lower residue, whereas RTC-EtOH exhibited the opposite trend, with lower weight loss and higher residue. These findings suggest that using a combination of sucrose and glucose as carbon sources tends to increase the second-stage weight loss while reducing the residual content. In contrast, the addition of ethanol appears to reduce the weight loss and increase the residue in BC samples.

This study's findings comparable to previous research. BC from *A. xylinum* AGR 60 exhibited a first-stage mass loss of 6%, a second-stage loss of 74%, and a residue of 20% at 700°C, with major decomposition between 300°C and 360°C (Potivara and Phisalaphong 2019). BC produced by *G. xylinus* AGR 60 showed a first-stage loss of 6.2%, a second-stage loss of 64.0%, and a residue of 22.8% at 600°C (Jenkhongkarn and Phisalaphong 2023). BC produced from various carbon sources, including glucose, fructose, sucrose, and glycerol, had residuals at 600°C ranging from 15.2% to 23.1% and a similar decomposition pattern (Tureck et al. 2021). In contrast, BC from kombucha fermentation of green tea showed three decomposition stages at 152°C, 267°C, and 359°C, with a total weight loss of 74.42% and 25.58% residue (Lima et al. 2023), differing from the two-stage decomposition observed in this study.

Table 4.15 Detail parameter of TGA/DTG analysis of BC samples from optimized kombucha

Samples	First stage weight loss (%)	Second stage weight loss (%)	Residue (%)	DTG Peak range (°C)	DTG T_{Max} (°C)
RTC-V1	5.62	70.69	23.66	272 – 378	336.50
RTC-V46	5.25	69.70	25.02	266 – 378	323.50
RTC-V53	7.47	71.35	21.14	260 – 378	333.33
RTC-C	6.03	71.01	23.01	265 – 380	353.67

The DTG T_{Max} results demonstrate the impact of carbon sources on the thermal stability of BC. In this study, optimized BC samples (RTC-V1, RTC-V46, RTC-V53) showed lower DTG T_{Max} values (336.50°C, 323.50°C, and 333.33°C, respectively)

compared to RTC-C (353.67°C). In previous experiments reported in the earlier chapter, RTC-SGlu exhibited a higher DTG T_{Max} (356.83°C) than RTC-C, while RTC-EtOH showed a lower value (347.50°C), suggesting that sucrose-glucose combinations improve thermal stability, whereas ethanol reduces it. For comparison, prior studies reported DTG T_{Max} values of 328.36°C for BC produced by *G. xylinus* (Jia et al. 2017), 354.5°C–355.4°C for BC from *G. hansenii* in HS medium (Vasconcellos and Farinas 2018), BC produced by *K. medellinensis* from various waste and agricultural by-products exhibits DTG T_{Max} values ranging from 327°C to 368°C (Molina-Ramírez et al. 2018a), and 366°C for kombucha-fermented green tea BC (Lima et al. 2023). These findings indicate that both carbon source combinations and fermentation conditions influence BC's thermal properties.

6) Mechanical Properties Analysis Using Nanoindentation

In this study, the sample of BC from RTC-V1 as the most suggested formulation is selected as representative of the optimized BC sample. RTC-C sample is included as a control for comparison. The detailed findings are summarized in **Table 4.16**. This table shows that the optimized BC sample (RTC-V1) exhibits no significant differences in mechanical properties compared to the control sample (RTC-C) across all parameters. Similarly, in the previous chapter, BC produced using a sucrose-glucose combination as the carbon source (RTC-SGlu) also showed no significant differences from RTC-C, while BC produced with ethanol as an additive (RTC-EtOH) displayed the highest number of parameters that were not significantly different from RTC-C. These findings suggest that using sucrose-glucose or ethanol as additives does not significantly impact the mechanical properties of BC produced from Thai red tea kombucha fermentation.

The Young’s modulus values observed in this study fall within a wide range, similar to those reported in previous research, with some values being lower or higher than others. For example, BC produced from various *Komagataeibacter* strains showed a range of 1.10 to 5.56 GPa (Chen et al. 2018a), while BC from different

strains and drying methods exhibited values between 198 and 659 MPa (Zeng et al. 2014). BC produced by *A. xylinum* E25 under static and rotating cultivation conditions showed Young's modulus values of 2.7 GPa and 0.3 GPa, respectively (Krystynowicz et al. 2002). Some studies report even higher values, such as *A. xylinum* AGR60 in coconut water, which achieved a Young's modulus of 9.14 GPa (Potivara and Phisalaphong 2019), and BC from kombucha fermentation, which reached 8.0 ± 1.9 GPa (Oliver-Ortega et al. 2021).

Table 4.16 Mechanical properties data analysis using nano-indenter of BC from kombucha fermentation of RTC-V1 and RTC-C.

Sample	MD (nm)	Pl (nm)	ML (mN)	H (GPa)	RM (GPa)	ERP	CC (nm/mN)	PW (nJ)	EW (nJ)	YM (GPa)
RTC-V1	3534.23 ±565.98	3124.20 ±567.15	50.10 ±0.00	0.22 ±0.09	5.10 ±1.08	0.14 ±0.03	10.91 ±0.85	54.78 ±7.74	19.64 ±1.29	4.66 ±0.99
RTC-C	3412.25 ±259.56	2980.18 ±253.91	50.10 ±0.00	0.22 ±0.05	4.94 ±0.56	0.15 ±0.01	11.50 ±0.22	54.41 ±4.64	20.80 ±0.47	4.51 ±0.51

MD: maximum depth, Pl: plastic, ML: maximum load, H: hardness, RM: reduced modulus, ERP: elastic recovery parameters, CC: contact compliance, PW: plastic work, EW: elastic work, and YM: Young's Modulus. Based on the statistical analysis, there were no significant differences among the samples across all parameters ($P < 0.05$).

4.5 Conclusion

This study employed Central Composite Design–Response Surface Methodology (CCD-RSM) to optimize BC (BC) production from Thai red tea kombucha. The effects and interactions of sucrose–glucose, tea, and ethanol concentrations were evaluated in relation to wet yield, dry yield, and WHC.

Although the model exhibited some limitations—such as relatively low R^2, adjusted R^2, predicted R^2 values, and a significant lack of fit—the quadratic model was still considered relevant. This is due to its theoretical suitability for capturing nonlinear effects and identifying potential optimal thresholds. Furthermore, the adequate precision value indicated that the model possessed an acceptable signal-to-noise ratio for predictive purposes.

Three formulations were selected from the optimization results for validation: RTC-V1 (the most recommended by the model), RTC-V46 (predicted to produce the highest yield), and RTC-V53 (predicted to produce the lowest yield). The validation results showed wet yields of 593.88 ± 39.27 to 658.66 ± 34.91 g/L, dry yields of 5.09 ± 0.92 to 5.56 ± 0.50 g/L, and WHC of 107.32 ± 8.01 to 115.60 ± 17.24 g water/g cellulose. No significant differences were observed among the three formulations, and all results fell within the predicted ranges, confirming the model's validity.

Characterization of the optimized BC further confirmed its quality. SEM analysis revealed uniform nanofiber networks with larger diameters (37.85–38.87 nm) compared to the control (30.65 nm). FTIR and XRD analyses indicated high crystallinity indices (83.23%–85.97%) and crystallite sizes ranging from 3.19 to 3.33 nm. Thermal analysis (TGA) showed lower DTG T_{max} values, while mechanical properties remained comparable across samples.

In conclusion, CCD-RSM proved to be an effective strategy for optimizing BC production from Thai red tea kombucha fermentation. Despite certain model

limitations, the approach yielded robust, reproducible, and scalable results, highlighting its strong potential for future industrial applications.

4.6 References

Agustin S, Wahyuni ET, Suparmo, et al (2021) Production and characterization of bacterial cellulose-alginate biocomposites as food packaging material. Food Res 5:204–210. https://doi.org/10.26656/fr.2017.5(6).733

Amarasekara AS, Wang D, Grady TL (2020) A comparison of kombucha SCOBY bacterial cellulose purification methods. SN Appl Sci 2:1–7. https://doi.org/10.1007/s42452-020-1982-2

Andritsou V, De Melo EM, Tsouko E, et al (2018) Synthesis and Characterization of Bacterial Cellulose from Citrus-Based Sustainable Resources. ACS Omega 3:10365–10373. https://doi.org/10.1021/acsomega.8b01315

Aswini K, Gopal NO, Uthandi S (2020) Optimized culture conditions for bacterial cellulose production by Acetobacter senegalensis MA1. BMC Biotechnol 20:1–16. https://doi.org/10.1186/s12896-020-00639-6

Azeredo HMC, Barud H, Farinas CS, et al (2019) Bacterial Cellulose as a Raw Material for Food and Food Packaging Applications. Front Sustain Food Syst 3:. https://doi.org/10.3389/fsufs.2019.00007

Balistreri GN, Campbell IR, Li X, et al (2024) Bacterial cellulose nanoparticles as a sustainable drug delivery platform for protein-based therapeutics. RSC Appl Polym 2:172–183. https://doi.org/10.1039/d3lp00184a

Barja F (2021) Bacterial nanocellulose production and biomedical applications. J Biomed Res 35:310–317. https://doi.org/10.7555/JBR.35.20210036

Bizeau J, Mertz D (2021) Design and applications of protein delivery systems in nanomedicine and tissue engineering. Adv Colloid Interface Sci 287:. https://doi.org/10.1016/j.cis.2020.102334

Brandes R, De Souza L, Carminatti C, Recouvreux D (2020) Production with a High

Yield of Bacterial Cellulose Nanocrystals by Enzymatic Hydrolysis. Int J Nanosci 19:1–8. https://doi.org/10.1142/S0219581X19500157

Cavicchia LOA, de Almeida MEF (2022) Health benefits of Kombucha: drink and its biocellulose production. Brazilian J Pharm Sci 58:1–13. https://doi.org/10.1590/s2175-97902022e20766

Cazón P, Vázquez M (2021) Improving bacterial cellulose films by ex-situ and in-situ modifications: A review. Food Hydrocoll 113:1–9. https://doi.org/10.1016/j.foodhyd.2020.106514

Charoenrak S, Charumanee S, Sirisa-ard P, et al (2023) Nanobacterial Cellulose from Kombucha Fermentation as a Potential Protective Carrier of Lactobacillus plantarum under Simulated Gastrointestinal Tract Conditions. Polymers (Basel) 15:. https://doi.org/10.3390/polym15061356

Chen S-Q, Lopez-Sanchez P, Wang D, et al (2018) Mechanical properties of bacterial cellulose synthesised by diverse strains of the genus Komagataeibacter. Food Hydrocoll 1–25. https://doi.org/10.1016/j.foodhyd.2018.02.031.This

Fatima A, Ortiz-Albo P, Neves LA, et al (2023) Biosynthesis and characterization of bacterial cellulose membranes presenting relevant characteristics for air/gas filtration. J Memb Sci 674:. https://doi.org/10.1016/j.memsci.2023.121509

Fei S, Yang X, Xu W, et al (2023) Insights into Proteomics Reveal Mechanisms of Ethanol-Enhanced Bacterial Cellulose Biosynthesis by Komagataeibacter nataicola. Fermentation 9:1–14. https://doi.org/10.3390/fermentation9060575

Fuller ME, Andaya C, McClay K (2018) Evaluation of ATR-FTIR for analysis of bacterial cellulose impurities. J Microbiol Methods 144:145–151. https://doi.org/10.1016/j.mimet.2017.10.017

Gaspar D, Fernandes SN, De Oliveira AG, et al (2014) Nanocrystalline cellulose applied simultaneously as the gate dielectric and the substrate in flexible field effect transistors. Nanotechnology 25:. https://doi.org/10.1088/0957-4484/25/9/094008

Gayathri G, Srinikethan G (2019) Bacterial Cellulose production by K. saccharivorans

BC1 strain using crude distillery effluent as cheap and cost effective nutrient medium. Int J Biol Macromol 138:950–957. https://doi.org/10.1016/j.ijbiomac.2019.07.159

Gismatulina YA, Budaeva V V. (2024) Cellulose Nitrates-Blended Composites from Bacterial and Plant-Based Celluloses. Polymers (Basel) 16:. https://doi.org/10.3390/polym16091183

Hegde S, Bhadri G, Narsapur K, et al (2013) Statistical Optimization of Medium Components by Response Surface Methodology for Enhanced Production of Bacterial Cellulose by Gluconacetobacter persimmonis. J Bioprocess Biotech 04:1–5. https://doi.org/10.4172/2155-9821.1000142

Heydorn RL, Lammers D, Gottschling M, Dohnt K (2023) Effect of food industry by-products on bacterial cellulose production and its structural properties. Cellulose 30:4159–4179. https://doi.org/10.1007/s10570-023-05097-9

Hossen MT, Kundu CK, Pranto BRR, et al (2024) Synthesis, characterization, and cytotoxicity studies of nanocellulose extracted from okra (Abelmoschus Esculentus) fiber. Heliyon 10:e25270. https://doi.org/10.1016/j.heliyon.2024.e25270

Illa MP, Khandelwal M, Sharma CS (2019) Modulated Dehydration for Enhanced Anodic Performance of Bacterial Cellulose derived Carbon Nanofibers. ChemistrySelect 4:6642–6650. https://doi.org/10.1002/slct.201901359

Jenkhongkarn R, Phisalaphong M (2023) Effect of Reduction Methods on the Properties of Composite Films of Bacterial Cellulose-Silver Nanoparticles. Polymers (Basel) 15:. https://doi.org/10.3390/polym15142996

Jia Y, Wang X, Huo M, et al (2017) Preparation and characterization of a novel bacterial cellulose/chitosan bio-hydrogel. Nanomater Nanotechnol 7:1–8. https://doi.org/10.1177/1847980417707172

Jittaut P, Hongsachart P, Audtarat S, Dasri T (2023) Production and characterization of bacterial cellulose produced by Gluconacetobacter xylinus BNKC 19 using

agricultural waste products as nutrient source. Arab J Basic Appl Sci 30:221–230. https://doi.org/10.1080/25765299.2023.2172844

Kazemi M, Faranak, Doosthoseini K, Azin M (2015) Effect of Ethanol and Medium on Bacterial Cellulose (Bc) Production By Gluconacetobacter Xylinus (Ptcc 1734). Cellul Chem Technol 49:455–462

Krystynowicz A, Czaja W, Wiktorowska-Jezierska A, et al (2002) Factors affecting the yield and properties of bacterial cellulose. J Ind Microbiol Biotechnol 29:189–195. https://doi.org/10.1038/sj.jim.7000303

Leonarski E, Cesca K, Zanella E, et al (2021) Production of kombucha-like beverage and bacterial cellulose by acerola byproduct as raw material. Lwt 135:1–8. https://doi.org/10.1016/j.lwt.2020.110075

Lima NF, Maciel GM, Fernandes I de AA, Haminiuk CWI (2023) Optimising the Production Process of Bacterial Nanocellulose: Impact on Growth and Bioactive Compounds. Food Technol Biotechnol 61:494–504. https://doi.org/10.17113/ftb.61.04.23.8182

Mohamad S, Abdullah LC, Jamari SS, et al (2022) Production and Characterization of Bacterial Cellulose Nanofiber by Acetobacter Xylinum 0416 Using Only Oil Palm Frond Juice as Fermentation Medium. J Nat Fibers 19:16005–16016. https://doi.org/10.1080/15440478.2022.2140243

Mohammad NH, El-Sherbiny GM, Hammad AA, et al (2021) Optimization of bacterial cellulose production using Plackett-Burman and response surface methodology. Egypt J Med Microbiol 30:93–101. https://doi.org/10.21608/EJMM.2021.197467

Molina-Ramírez C, Castro C, Zuluaga R, Gañán P (2018a) Physical Characterization of Bacterial Cellulose Produced by Komagataeibacter medellinensis Using Food Supply Chain Waste and Agricultural By-Products as Alternative Low-Cost Feedstocks. J Polym Environ 26:830–837. https://doi.org/10.1007/s10924-017-0993-6

Molina-Ramírez C, Enciso C, Torres-Taborda M, et al (2018b) Effects of alternative

energy sources on bacterial cellulose characteristics produced by Komagataeibacter medellinensis. Int J Biol Macromol 117:735–741. https://doi.org/10.1016/j.ijbiomac.2018.05.195

Nguyen TA, Nguyen XC (2022) Bacterial Cellulose-Based Biofilm Forming Agent Extracted from Vietnamese Nata-de-Coco Tree by Ultrasonic Vibration Method: Structure and Properties. J Chem 2022:1–10. https://doi.org/10.1155/2022/7502796

Oliver-Ortega H, Geng S, Espinach FX, et al (2021) Bacterial cellulose network from kombucha fermentation impregnated with emulsion-polymerized poly(Methyl methacrylate) to form nanocomposite. Polymers (Basel) 13:1–17. https://doi.org/10.3390/polym13040664

Padmanabhan SK, Lamanna L, Friuli M, Licciulli A (2023) Carboxymethylcellulose-Based Hydrogel Obtained from Bacterial Cellulose. Molecules 28:1–10. https://doi.org/https://doi.org/10.3390/molecules28020829

Pandey A, Singh A, Singh MK (2024) Novel low-cost green method for production bacterial cellulose. Polym Bull 81:6721–6741. https://doi.org/10.1007/s00289-023-05023-w

Pham TT, Tran TTA (2023) Evaluation of the Crystallinity of Bacterial Cellulose Produced from Pineapple Waste Solution by Using Acetobacter Xylinum. ASEAN Eng J 13:81–91. https://doi.org/10.11113/aej.V13.18868

Potivara K, Phisalaphong M (2019) Development and characterization of bacterial cellulose reinforced with natural rubber. Materials (Basel) 12:. https://doi.org/10.3390/ma12142323

Rachtanapun P, Jantrawut P, Klunklin W, et al (2021) Carboxymethyl bacterial cellulose from nata de coco: Effects of NaOH. Polymers (Basel) 13:1–17. https://doi.org/10.3390/polym13030348

Rahmayetty, Sulaiman F (2023) Wastewater from the Arenga Starch Industry as a Potential Medium for Bacterial Cellulose and Cellulose Acetate Production.

Polymers (Basel) 15:1–15. https://doi.org/10.3390/polym15040870

Raiszadeh-Jahromi Y, Rezazadeh-Bari M, Almasi H, Amiri S (2020) Optimization of bacterial cellulose production by Komagataeibacter xylinus PTCC 1734 in a low-cost medium using optimal combined design. J Food Sci Technol 57:2524–2533. https://doi.org/10.1007/s13197-020-04289-6

Ramírez Tapias YA, Di Monte MV, Peltzer MA, Salvay AG (2022) Bacterial cellulose films production by Kombucha symbiotic community cultured on different herbal infusions. Food Chem 372:. https://doi.org/10.1016/j.foodchem.2021.131346

Revin V, Liyaskina E, Nazarkina M, et al (2018) Cost-effective production of bacterial cellulose using acidic food industry by-products. Brazilian J Microbiol 49:151–159. https://doi.org/10.1016/j.bjm.2017.12.012

Rodrigues AC, Fontão AI, Coelho A, et al (2019) Response surface statistical optimization of bacterial nanocellulose fermentation in static culture using a low-cost medium. N Biotechnol 49:19–27. https://doi.org/10.1016/j.nbt.2018.12.002

Said Azmi SNN, Samsu Z 'Asyiqin, Mohd Asnawi ASF, et al (2023) The production and characterization of bacterial cellulose pellicles obtained from oil palm frond juice and their conversion to nanofibrillated cellulose. Carbohydr Polym Technol Appl 5:100327. https://doi.org/10.1016/j.carpta.2023.100327

Samuel OS, Adefusika AM (2019) Influence of Size Classifications on the Structural and Solid-State Characterization of Cellulose Materials. In: Pascual R, Martín MEE (eds) Cellulose. IntechOpen

Sardjono SA, Suryanto H, Aminnudin, Muhajir M (2019) Crystallinity and morphology of the bacterial nanocellulose membrane extracted from pineapple peel waste using high-pressure homogenizer. In: AIP Conference Proceedings. AIP Publishing, pp 080015-1-080015–5

Singh O, Panesar PS, Chopra HK (2017) Response surface optimization for cellulose

production from agro industrial waste by using new bacterial isolate Gluconacetobacter xylinus C18. Food Sci Biotechnol 26:1019–1028. https://doi.org/10.1007/s10068-017-0143-x

Singhsa P, Narain R, Manuspiya H (2018) Physical structure variations of bacterial cellulose produced by different Komagataeibacter xylinus strains and carbon sources in static and agitated conditions. Cellulose 25:1571–1581. https://doi.org/10.1007/s10570-018-1699-1

Srivastava S, Mathur G (2022) Komagataeibacter saccharivorans strain BC-G1: an alternative strain for production of bacterial cellulose. Biologia (Bratisl) 77:3657–3668. https://doi.org/10.1007/s11756-022-01222-4

Teixeira SRZ, Dos Reis EM, Apati GP, et al (2019) Biosynthesis and functionalization of bacterial cellulose membranes with cerium nitrate and silver nanoparticles. Mater Res 22:1–13. https://doi.org/10.1590/1980-5373-MR-2019-0054

Thielemans K, De Bondt Y, Comer L, et al (2023) Decreasing the Crystallinity and Degree of Polymerization of Cellulose Increases Its Susceptibility to Enzymatic Hydrolysis and Fermentation by Colon Microbiota. Foods 12:1100. https://doi.org/10.3390/foods12051100

Thorat MN, Dastager SG (2018) High yield production of cellulose by a: Komagataeibacter rhaeticus PG2 strain isolated from pomegranate as a new host. RSC Adv 8:29797–29805. https://doi.org/10.1039/c8ra05295f

Tureck BC, Hackbarth HG, Neves EZ, et al (2021) Obtaining and characterization of bacterial cellulose synthesized by Komagataeibacter hansenii from alternative sources of nitrogen and carbon. Rev Mater 26:. https://doi.org/10.1590/S1517-707620210004.1392

Vasconcellos VM, Farinas CS (2018) The effect of the drying process on the properties of bacterial cellulose films from gluconacetobacter hansenii. Chem Eng Trans 64:145–150. https://doi.org/10.3303/CET1864025

Wang SS, Han YH, Chen JL, et al (2018) Insights into bacterial cellulose biosynthesis

from different carbon sources and the associated biochemical transformation pathways in Komagataeibacter sp. W1. Polymers (Basel) 10:. https://doi.org/10.3390/polym10090963

Yanti NA, Ahmad SW, Muhiddin NH (2018) Evaluation of inoculum size and fermentation period for bacterial cellulose production from sago liquid waste. J Phys Conf Ser 1116:. https://doi.org/10.1088/1742-6596/1116/5/052076

Yao H, Dai Q, You Z (2015) Fourier Transform Infrared Spectroscopy characterization of aging-related properties of original and nano-modified asphalt binders. Constr Build Mater 101:1078–1087. https://doi.org/10.1016/j.conbuildmat.2015.10.085

Yilmaz M, Goksungur Y (2024) Optimization of Bacterial Cellulose Production from Waste Figs by Komagataeibacter xylinus. Fibers 12:1–18. https://doi.org/10.3390/fib12030029

Zeng M, Laromaine A, Roig A (2014) Bacterial cellulose films: influence of bacterial strain and drying route on film properties. Cellulose 21:4455–4469. https://doi.org/10.1007/s10570-014-0408-y

Zeng X, Liu J, Chen J, et al (2011) Screening of the common culture conditions affecting crystallinity of bacterial cellulose. J Ind Microbiol Biotechnol 38:1993–1999. https://doi.org/10.1007/s10295-011-0989-5